A review of field-aligned beams observed upstream of the bow shock

Karim Meziane*, M. Wilber†, C. Mazelle**, G.K. Parks† and A.M. Hamza*

*University of New Brunswick, Fredericton
†Space Sciences Laboratory, U. California, Berkeley
**Centre d'Etude Spatiale des Rayonnements, Toulouse

Abstract. For more than two decades the Earth's bow shock and traveling interplanetary shocks have attracted much attention as researchers have attempted to understand the collisionless mechanisms that thermalize transmitted particles and accelerate those that are observed propagating away from the shock into the upstream. We are concerned here with the class of particles emerging from the shock that are field-aligned and have energies of a few to several keV, and base our results on observations primarily from the Earth's foreshock. While the basic empirical picture has been known for some time, fundamental questions about the underlying mechanisms producing them have resisted a comprehensive explanation. This review talk will begin with an overview of the observational framework, along with selected new results. The latter include recent refinements in the characterizations of upstream field-aligned beams as a function of the shock geometry parameter θ_{Bn}. Other observations from the Cluster spacecraft have shown the occurence of a very sharp boundary separating FABs and gyrating ion populations in the foreshock. The Wind spacecraft has seen FABs at distances in excess of $\sim$100 R_E from the Earth, indicating lifetimes greater than expected from linear theory of the ion-ion streaming instability. These observations prompt new questions. Some analytic calculations will be reviewed briefly. Models based upon the guiding center approximation and those which introduce diffusion as a means of enhancing the fluxes of upstream beams fail to produce the properties observed.

Keywords: foreshock, ion, acceleration, quasiperpendicular, shock
PACS: 96.50.Ek, 96.50.Pw

INTRODUCTION

It is now well-known that broad classes of upstream distributions associated with sunward propagating ions are commonly observed upstream of the Earth's bow shock [1]. Our interest in the present paper is with field-aligned ion beams (FABs), which consist of ions collimated along the interplanetary magnetic field (IMF). Although significant observations and investigations, including theoretical studies [2, 3] and simulations [4] have been carried out in the previous years, their production mechanisms remain an open issue [5]. Understanding the production mechanism responsible for coherent particle distributions is of fundamental importance in shock acceleration since it is intimately associated with the particle injection problem at quasi-perpendicular shocks. High quality data are now available from recent spacecraft such as Cluster that allow for detailed quantitative studies and the deconvolution of spatial and temporal variations. In this paper we present new observations briefly, and indicate how production mechanisms currently proposed cannot explain these observations.

CP 781, *The Physics of Collisionless Shocks,* edited by G. Li, G. P. Zank, and C. T. Russell

EARLY OBSERVATIONS

Observations describing the basic properties of FABs, based on 2-D particle instrumentation, have been extensively reported during the ISEE era [6]. Typically, field-aligned ion beams are observed upstream of quasi-perpendicular shocks characterized by $40^\circ \lesssim \theta_{Bn} \lesssim 70^\circ$, where θ_{Bn} is the angle between the interplanetary magnetic field direction and the local bow shock normal. Their bulk energy is typically few keV and the energy spectrum rarely extends beyond ~ 15 keV. Their bulk speeds, ranging from one to several times the solar wind speed, have been satisfactorily measured and are well correlated with the angle θ_{Bn} [7]. Downstream of the FAB region intermediate ion distributions are observed to have a kidney-shape that is symmetric across the magnetic field direction. These distributions are always observed in association with large amplitude ($\Delta B/B \sim 1$), weakly compressive, nearly monochromatic, ULF ($\omega/\Omega_i \ll 1$) waves [8]. These waves propagate along the ambient magnetic field direction [9, 10]. The large amplitude ULF waves have not been observed with FABs. However, whistler-like waves (commonly called foreshock 1-Hz waves) having small-amplitude $\Delta B/B \sim 0.1$ are occasionally observed in association with FABs [9, 11]. Carefull examination of the ion energy-spectrogram showed that the foreshock 1-Hz waves are more often observed with "spread" FABs rather than with the "narrow" ones [11]. From case examples, it seems that the energy spread occurs at a lower energy. Early field aligned beam temperature determinations provided an average value of 345 km s^{-1}, which may extend up to ~ 800 km s^{-1} [6]. The temperature anisotropy $T_\perp/T_\parallel$ is in the range of 4–9 [1]. Based upon particle features alone, the distinction between the FABs and intermediate distributions is quite arbitrary; the main criterion to distinguish the two populations is the lack or presence of large-aplitude ULF waves. However, it is not unusual to see very small amplitude ULF waves in association with the FABs.

It is worthy of mention that the FABs are considered the most important source of free energy in the foreshock region. The resulting ion distribution (FAB superposed on the solar wind) is susceptible to numerous instabilities. The electromagnetic ion-ion cyclotron instability, discussed in detail by Gary et al. [12], has the highest linear growth rate. Both the parallel and the oblique modes are unstable for a large range of FAB speeds, and both are in cyclotron resonance with FABs; the parallel case has the maximum growth rate. The resonant parallel mode has been successfully indentified in detailed case studies, which showed that the ULF waves observed in association with gyrating ion distributions are actually in cyclotron resonance with adjacent FABs [10, 13].

RECENT OBSERVATIONS

Theory and simulation models [14] predict that, due to electromagnetic instabilities briefly mentioned above, a typical FAB is heated and becomes an intermediate-like distribution after $\sim 25/\Omega_i$. We may then expect a cut-off distance on the order of $\sim 30\, R_E$ from the shock. Figure 1 from WIND/3DP shows examples of particle distributions having 15 keV FABs observed at $\sim 93\, R_E$ from Earth. (Presented in the plasma frame, the main beam in the center is the solar wind.) The FABs are travelling opposite

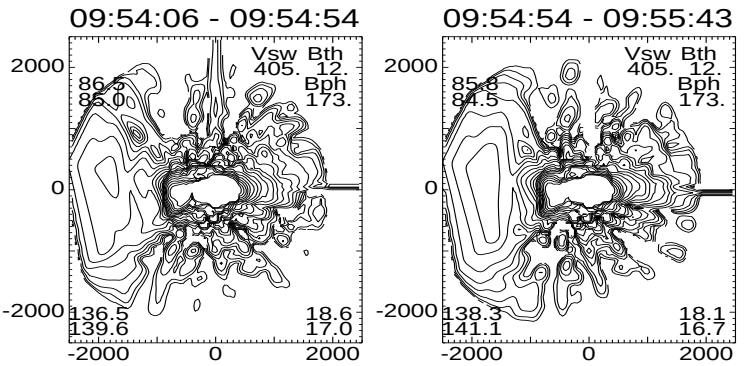

FIGURE 1. Wind/3DP ion measurements of FABs on 28 August 1995 at 93 R_E.

to **B** (left of center, with pitch angles extending to 45°. Several similar distributions have been observed at $\sim 100\ R_E$ and beyond. Clearly, these beams are unexpected at such large distances from the shock. Work is now in progress to establish their source characteristics and to understand how they reach far upstream regions.

We have examined in detail the properties of field aligned beams as a function of shock geometry, taking special care to isolate the influences of θ_{Bn} from other parameters [15]. Simple kinematic arguments lead to expectations that densities and beam speeds will vary with θ_{Bn}, although no temperature relation immediately follows. Figure 2 shows moments computed for successive FABs observed by the Cluster/CIS experiment on 23 April 2001, 0647–0651 UT. During the interval of interest no ULF waves were observed and the IMF direction was slowly rotating toward a less radial configuration. As selected, the only parameter that changed significantly for this event was the angle θ_{Bn}. Successive panels show θ_{Bn} variation of the beam density normalized to the solar wind density (Figure 2a), the beam speed normalized to the solar wind speed (Figure 2b), and beam parallel and perpendicular temperatures (Figure 2c). Clearly the beam properties are remarkably well correlated with the shock geometry. The strong decrease in beam densities with θ_{Bn} shown in Figure 2a is expected, since only those particles moving upstream in the de Hoffman-Teller frame will avoid re-encounter with the shock. The increase in the frame transformation velocity as θ_{Bn} increases requires that the beams originate from further in the tail of the source distribution. The plateau in *n* seen toward the left of Figure 2a suggests that the beam production mechanism breaks down for a critical value of θ_{Bn}. Detailed study of other events are now underway to verify the occurence of this density-plateau relation.

Figure 2b shows that the acceleration increases linearly with $\cos\theta_{vn}/\cos\theta_{Bn}$, where θ_{vn} is the angle the shock normal makes with the direction of the solar wind flow. Similar results have been obtained in an early study [2]. We mention here that the beam speed is given in the plasma frame of reference. The $\cos\theta_{vn}/\cos\theta_{Bn}$ factor appears in the expression for the de Hoffman-Teller frame speed V_S expressed in the plasma rest frame: $V_S = -v_{sw}\cos\theta_{Bn}/\cos\theta_{vn}$. During the time interval presented above, θ_{vn} remains nearly constant. According to the kinematic description of ion reflection by Sonnerup [16], the post encounter speeds are given by $V_B = -(1+\delta)V_S$, where δ is a coefficient indicating

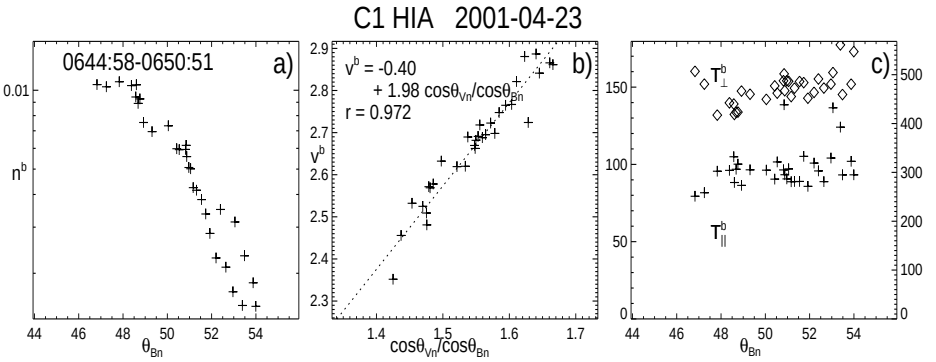

FIGURE 2. Moments determined for FABs on 23 April 2001. a) $n = n_b/n_{sw}$ *vs.* θ_{Bn}.; b) $v = v_b/v_{sw}$ *vs.* $\cos\theta_{vn}/\cos\theta_{Bn}$; c) $T_\parallel$ *vs.* θ_{Bn}('+'s, left axis with units of eV) and $T_\perp$ *vs.* θ_{Bn}(diamonds, right axis).

the degree to which the particle magnetic moment is conserved ($\delta = 1$ for the adiabatic case).

In Figure 2c (which has the scale for $T_\parallel$ on the left axis, and that for $T_\perp$ on the right) the temperature anisotropy $T_\perp/T_\parallel$ is a little lower than 5, and within the range of 4–9 quoted above. Most notable is that there is no clear dependence of either temperature upon θ_{Bn}. This and other cases suggest, if anything, a weak increase in $T_\perp$ with θ_{Bn}. A straightforward view might be that the perpendicular temperature should reflect the free-escape conditions for particles in a source distribution just exterior to the shock. In that case, however, we should expect [15] $T_\perp \sim 1/\sin^2\theta_{Bn}$, which, rather than increasing, should decrease by $\sim$ 20% over this range of θ_{Bn}. This is a topic of ongoing investigation.

The different types of populations observed upstream of the bow shock are located in distinct foreshock regions. FABs are seen in a layer of $\sim 0.4\ R_E$ thickness, followed further downstream by a $\sim\ 3.5R_E$-wide layer of intermediate ions [7]. Gyrophase-bunched ions, characterized by a bulk motion at non-zero pitch angles, can be found along the upstream edge of the intermediate region. This implies the existence of a spatial boundary separating the different types of populations. Previously Greenstadt and Baum [17] showed a spatial boundary separating regions where ULF waves are present from those where thay are absent. Subseqently, Le and Russell [18] found a similar boundary, but its statistical average slope differed signifi cantly. However, it is diffi cult to resolve transitions between different foreshock regions due to the rapid rate of IMF rotations.

More recently, we reported the presence of a sharp spatial boundary separating FABs from gyrating ions using observations from the Cluster spacecraft. Figure shows successive spectra from CIS/CODIF on spacecraft 1, which indicate an apparent merging of an energetic population with FABs. Detailed examination of the 3D distributions showed that the energetic component was a remotely-sensed gyrating population[19]. Figure is a schematic illustrating the remote sensing model accounting for the two-peak spectra seen near 2111 UT. The spacecraft is located at S and observes FABs travelling along the fi eld line threading it. Simultaneously, it detects gyrating ions at high energy having

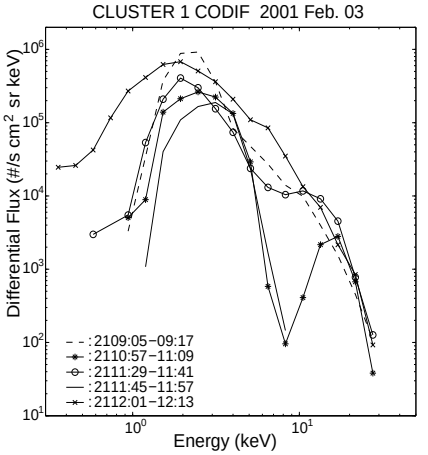

FIGURE 3. Spectra from CIS/CODIF for different times on 3 February 2001.

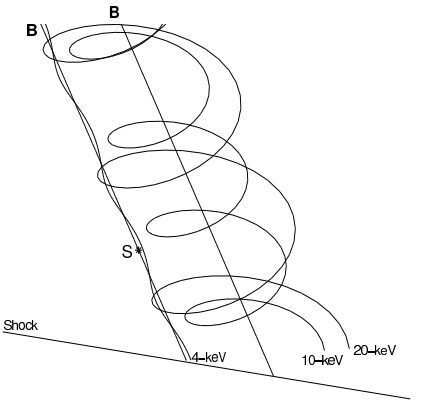

FIGURE 4. Remote-sensing schematic for 3 February 2001.

guiding centers along adjacent field lines separated by less than one ion gyroradius ρ_i. Figure 3 of Meziane et al. [19] shows that the energetic component initially appears in narrow range of gyrophase angles consistent with guiding centers downstream of the spacecraft. A direct inference from these observations was that the transition between the two types of populations occured within ~ 1 gyrating ion gyroradius. This boundary agreed with the ULF wave boundary observed by Le and Russell [18], and predicted theoretically [20]. We note, however, that the FABs observed along the boundary do not match quantitatively the emission mechanisms posited to occur at the shock.

PRODUCTION MECHANISMS FOR FABS

In this section we briefly discuss guiding center production mechanisms. A straightforward application of kinematic reflection theory, where energy and the first adiabatic invariant are conserved in the de Hoffman-Teller frame, leads to an expression relating a required initial particle energy to the observed final (beam) particle parameters, all in the plasma frame: $E_i = E_f[1 + 4(\frac{V_s}{v_f}^2 - \frac{V_s}{v_f}\cos\alpha)]$, where α is the pitch angle. Decker [21] showed that the energy gain for adiabatic reflection depends exclusively upon the shock strength B_2/B_1. Typical upstream values indicate an initial energy of 0.2–0.5 keV, far greater than the typical energies of the presumed solar wind source. Similar reasoning can be applied to adiabatic leakage of particles from the magnetosheath, but this produces fluxes lower than those observed by an order of magnitude [22]. Generalizing the problem to allow for non-conservation of first adiabatic invariant or loss of energy does not improve the situation.

Researchers have attempted to reconcile the inadequacies of guiding center models by considering diffusive processes. One scenario that is receiving a lot of attention includes strong cross-field diffusion of particles within magnetic field turbulence [23].

Scattering occuring on time scales smaller than a gyroperiod repeatedly return particles to the upstream, permitting additional opportunities to sample the strong electric field and consequent acceleration in the shock ramp. Hybrid and 1-D full-particle simulations [23] using thermal seed populations show that this approach produces upstream particle fluxes lower than observed by several orders of magnitude. Additional difficulties are a lack of physical motivation for the diffusion coefficients, which up until now have been applied in an *ad hoc* manner, and the unlikelihood of diffusion producing beams that are field aligned. Tanaka [24] modeled upstream ion production by noting that the temperature anisotropy in the magnetosheath drives strong electromagnetic ion cyclotron waves. Non-thermal gyrating particles, initially specularly reflected in the shock ramp, and subsequently crossing into the sheath were scattered by these waves, and those redirected back upstream were adiabatically folded in pitch angle as they cross the shock. While these models were able to produce fluxes comparable to those of the observed beams, the dependence upon θ_{Bn} found was the reverse of what was observed [15]. This dependence in turn was determined by the assumed gyrating particle profile. A recent idea [25] is that strong scattering of the gyrating particles instead occurs within the shock ramp, diffusing these particles into free-escape regions of velocity space, which are sufficient in number to provide the FABs. See Kucharek (this volume) for additional details.

ACKNOWLEDGMENTS

We thank the International Space Science Institute in Bern for their support of this work, and members of the ISSI Upstream Ions Collaboration for useful discussions. Work at UNB is supported by the Canadian Natural Science and Engineering Council. MW and GKP acknowledge support from NASA Grant NAG5-10131.

REFERENCES

1. G. Paschmann, N. Sckopke, I. Papamastorakis, J. R. Asbridge, S. J. Bame, and J. T. Gosling, *Journal of Geophysical Research*, **86**, 4355–4364 (1981).
2. G. Paschmann, N. Sckopke, J. R. Asbridge, S. J. Bame, and J. T. Gosling, *Journal of Geophysical Research*, **85**, 4689–4693 (1980).
3. M. F. Thomsen, S. J. Schwartz, and J. T. Gosling, *Journal of Geophysical Research*, **88**, 7843–7852 (1983).
4. D. Burgess, *Journal of Geophysical Research*, **92**, 1119–1130 (1987).
5. S. J. Schwartz, M. F. Thomsen, and J. T. Gosling, *Journal of Geophysical Research*, **88**, 2039–2047 (1983).
6. C. Bonifazi, and G. Moreno, *Journal of Geophysical Research*, **86**, 4381–4396 (1981a).
7. C. Bonifazi, and G. Moreno, *Journal of Geophysical Research*, **86**, 4397–4404 (1981b).
8. S. A. Fuselier, M. F. Thomsen, J. T. Gosling, S. J. Bame, and C. T. Russell, *Journal of Geophysical Research*, **91**, 91– (1986).
9. M. M. Hoppe, C. T. Russell, L. A. Frank, and E. W. Eastman, T. E.; Greenstadt, *Journal of Geophysical Research*, **86**, 4471–4492 (1981).
10. K. Meziane, C. Mazelle, R. P. Lin, D. LeQuéau, D. E. Larson, G. K. Parks, and R. P. Lepping, *Journal of Geophysical Research*, **106**, 5731–5742 (2001).
11. M. M. Hoppe, C. T. Russell, T. E. Eastman, and L. A. Frank, *Journal of Geophysical Research*, **87**, 643–650 (1982).
12. S. P. Gary, J. T. Gosling, and D. W. Forslund, *Journal of Geophysical Research*, **86**, 6691– (1981).

13. C. Mazelle, K. Meziane, D. Le Quéue, M. Wilber, J. P. Eastwood, H. Rème, J.-A. Sauvaud, J.-M. Bosqued, I. Dandouras, M. McCarthy, L. M. Kistler, B. Klecker, A. Korth, M. B. Bavassano-Cattaneo, R. Lundin, and A. Balogh, *Planetary and Space Science*, pp. 785–795 (2003).
14. D. Winske, and M. M. Leroy, *Journal of Geophysical Research*, **89**, 2673–2688 (1984).
15. M. Wilber, K. Meziane, G. K. Parks, L. M. Kistler, I. Dandouras, H. Rème, J.-A. Sauvaud, J.-M. Bosqued, M. McCarthy, B. Klecker, A. Korth, M.-B. Bavassano-Cattaneo, R. Lundin, and E. Lucek, *Annales Geophysicae* (2005), submitted, May 2005.
16. B. U. O. Sonnerup, *Journal of Geophysical Research*, **74**, 1301–1304 (1969).
17. E. W. Greenstadt, and L. W. Baum, *Journal of Geophysical Research*, **91**, 901– (1986).
18. G. Le, and C. T. Russell, *Planetary and Space Science*, **40**, 1203–1213 (1992).
19. K. Meziane, M. Wilber, C. Mazelle, D. LeQuéau, H. Kucharek, E. Lucek, J. A. Sauvaud, A. M. Hamza, H. Rème, J. M. Bosqued, I. Dandouras, G. K. Parks, M. McCarthy, B. Klecker, A. Korth, M.-B. Bavassano-Cattaneo, and R. Lundin, *Journal of Geophysical Research*, **109**, A05107, doi:10.1029/2003JA010374 (2004).
20. G. Skadron, R. T. Holdaway, and M. A. Lee, *Journal of Geophysical Research*, **93**, 11,354–11,362 (1988).
21. R. B. Decker, *Journal of Geophysical Research*, **88**, 9959–9973 (1983).
22. J. P. Edmiston, C. F. Kennel, and D. Eichler, *Geophysical Research Letters*, **9**, 531 (1982).
23. J. Giacolone, J. R. Jokipii, and J. Kóta, *Journal of Geophysical Research*, **99**, 19,351–19,358 (1994).
24. M. Tanaka, C. C. Goodrich, D. Winske, and K. Papadopoulos, *Journal of Geophysical Research*, **88**, 3046–3054 (1983).
25. H. a. Kucharek, *Annales Geophysica* (2004).